

Optimization of Dose to Patient in Diagnostic Radiology Using Monte Carlo Method

Massoud E and Diab HM*

Radiation Protection Department, Nuclear and Radiological Regulatory Authority, Cairo, Egypt

Abstract

Entrance Surface Dose (ESD) is one of the basic dosimetric quantities for measuring the patient dose and hence, an excellent tool for optimization purposes and for comparison with the international reference values. ESD value measurement for patient is also, an essential component of the quality assurance program for individual X-ray radiology departments. Factors affecting dose in all imaging modalities include beam energy, filtration, collimation, patient size, and image processing. Organ absorbed dose can be estimated by using a conversion factor along with a measured value of entrance exposure. When estimating the radiation dose of an individual patient, patient specific calculation methods can be used. The main objective of this study was to develop methods for assessment of ESD. In this study, image quality is quantified by modeling the whole X-ray imaging system, including the X-ray tube, and patient. This is accomplished by using Monte Carlo (MC) simulation methods that allow simultaneous estimates of measures of image quality and patient dose. In This study MCNP4C code was used to state a model for both human body and X-ray machine, to carry out such an investigation. Mathematical model of the human body with its all internal organs was used, and an image receptor of variable thickness and composition. Experimental results showed good agreement with theoretical predictions. The model may be used to generate data for a range of exposure conditions, and sample results will be presented. The usefulness and limitations of such a theoretical model will be discussed.

Keywords: Monte Carlo method; Diagnostic X-ray; ESD

Introduction

X-ray diagnostic machines-one of the most widely used man made radiation sources- are now part of any patient's life, after, before and also sometimes during treatment for any problem. There are fundamentally two reasons for measuring or estimating radiation doses to patients; firstly measurements provide a mean for setting and checking standards of good practice as an aid to the optimization patient protection. Secondly, estimates of the absorbed dose to tissues and organs in the patients are needed to determine the risks so that diagnostic technique can be properly justified and cases of accidental overexposure thoroughly investigated [1].

Information that can be utilized to give a patient an accurate diagnosis, and subsequently a successful treatment is essential. However, imaging with ionizing radiation is also associated with a small risk for cancer induction or genetic detriment. When X-ray photons are scattered or absorbed in the cells of the human body, ionizations occur that can alter molecular structures and thus do harm to the cell. The most important damage to the cell is damaged in the DNA since this may induce mutations. Ultimately, the damage may lead to that the cell is killed, and if enough cells are killed, the function of the tissue or organ will be deteriorated. This type of acute harm due to large radiation exposures is referred to as a deterministic effect [2]. However, at the relatively low radiation exposures in diagnostic radiology, the damages caused by ionizing radiation are often rather easily repaired. Yet, sometimes the damage on the DNA is more complex. This can cause mutations or chromosomal aberrations, which in turn may lead to a modified cell but with a retained reproduction capacity. In some cases, such modified cells can result in a cancer. In the case where the harmful effects of ionizing radiation are only known, statistically, it is referred as a stochastic effect. The risk related to stochastic effects to a human from exposure from ionizing radiation is often quantified with the effective dose, E [3]. The intensity and quality of the radiation emerging from an X-ray tube are primarily a function of the tube

current, exposure time, applied and filtration source quantities as identified in Figure 1. The most common method is the determination of the entrance surface dose using thermoluminescent dosimeters or calculating from the output of the X-ray unit and dose-area product. To insure the ESD without using these factors, Monte Carlo techniques for dose estimation to organs have been developed [4].

In this study, MCNP4C is used to simulate the diagnostic radiology X-ray tube with the aim of the predicting the X-ray spectra using various tube voltages (between 50 and 120 kV). The method, based on Monte Carlo technique, is integrated into flexible software capabilities to estimate the absorbed dose when the possibility of application of other actual methods does not exist.

Materials and Methods

Monte carlo codes

MCNP is a well-known general purpose Monte Carlo code for the transport of neutrons, photons and electrons developed at the Los Alamos National Laboratory. The user can apply up to second order surfaces (boxes, ellipsoids, cones, etc.) and fourth order tori to build a three-dimensional (3D) geometry, which can be filled with materials of arbitrary composition and density. Point, surface or volume sources

*Corresponding author: Diab HM, Nuclear and Radiological Regulatory Authority, 3 Ahmed El-Zomor Street, Nasr city, Cairo, Egypt, Tel: 00202 22740238; Fax: 00202 22740238; E-mail: hnndiab@yahoo.co.uk

Received December 30, 2013; Accepted January 29, 2014; Published January 31, 2014

Citation: Massoud E, Diab HM (2014) Optimization of Dose to Patient in Diagnostic Radiology Using Monte Carlo Method. J Cell Sci Ther 5: 155. doi:10.4172/2157-7013.1000155

Copyright: © 2014 Massoud E, et al. This is an open-access article distributed under the terms of the Creative Commons Attribution License, which permits unrestricted use, distribution, and reproduction in any medium, provided the original author and source are credited.

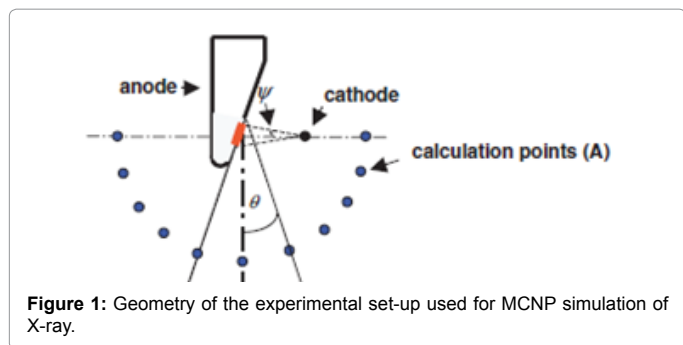


Figure 1: Geometry of the experimental set-up used for MCNP simulation of X-ray.

of radiation can be defined, from which the mentioned particles are emitted with user specified probability distributions for energy and direction. The code then simulates the particle tracks and interactions with the materials, according to probability density distributions implied by particle and material properties. Taking a comprehensive account of the underlying physics of radiation-matter interaction, it creates secondary particles (which are also transported) and keeps a record of quantities like particle fluence, energy deposition and dose. The user indicates at what points, surfaces or volumes, these quantities are reported. For this paper MCNP version 4C was used, which has been implemented on a Compaq XP900 Alpha workstation. Without attempting optimization, i.e. the application of additional variance reduction techniques, it typically takes some 6 h of computer processing time (20 million starting particles) to yield less than 0.5% relative statistical uncertainty in the calculated effective dose conversion factor for patients [5].

Monte Carlo calculations simulate and record the energy deposition of X-ray photons in mathematically described anthropomorphic phantoms. The radiation interaction histories of a large number of incident photons are followed using known physical descriptions of the interaction processes and the resulting energy depositions at the sites of interaction are recorded [6]. For diagnostic radiology dosimetry the physical process treated are limited to the photoelectric effect and Compton scattering since the initial photon energies in the range of the interest are less than 150 KeV [7]. The energy given to the secondary electrons is assumed to be absorbed at the same point, that is, the kerma is equal to the absorbed dose. The ranges of the secondary electrons are small compared with the dimensions of the study organs, and the absorbed dose does not change abruptly with distance except at the boundary where composition and density change [8]. These boundary effects have little impact in the determination of the average absorbed dose in the tissues. The one exception is the active bone marrow, where a small increase in absorbed dose due to the size of the marrow cavities is expected from increased photoelectron emission by surrounding bone [7,8].

Tissue doses are obtained by summing, in each organ, all energy depositions from primary and scattered photons, and dividing by the total organ mass. The result is the average absorbed dose in the entire organ regardless of the fraction of the organ.

The body is represented as erect with the positive z-axis directed upward toward the head. The x-axis is directed to the phantom's left, and the y-axis is directed toward the posterior side of the phantom. The origin is taken at the center of the base of the trunk section of the phantom [7].

This study presents a model for the human body that was done using MC technique. In Figure 2(a) the model as given by the output

of the used code is shown which was stated on that given in (b) [9], some of the organs such as spine, kidneys and the rest of the respiratory system do not appear according to the drawing section. The elemental compositions for all human organs and for the adipose tissue were derived from data in ICRP 89 [10]. As composition and tissue density are important parameters in determining the transport of photons in the body, geometric shape of each organ in the human body is very essential in preparing the input of the code concerning with the relation between all these organs and they must not intersect. Cristy [11], gave these mathematical representations for different ages.

Trunk: The trunk, exclusive of the female breasts, is represented by a solid elliptical cylinder specified by:

$$\left(\frac{x}{A_T}\right)^2 + \left(\frac{y}{B_T}\right)^2 \leq 1 \text{ and } 0 \leq z \leq C_T, \text{ where } A_T=17.25, B_T=9.80$$

and $C_T=63.10$

The trunk section includes the arms and the pelvic region to the crotch. The female breasts are appended to the outside of the trunk section.

Skull: The skull comprises the cranium and the facial skeleton. The cranium is represented by the volume between two concentric ellipsoids defined by:

$$\left(\frac{x}{a}\right)^2 + \left(\frac{y}{b}\right)^2 + \left(\frac{z-[C_T+C_{H1}]}{c}\right)^2 \geq 1$$

$$\text{And } \left(\frac{x}{a}\right)^0 + \left(\frac{y}{b}\right)^2 + \left(\frac{z-[C_T+C_{H1}]}{c}\right)^2 \geq 1$$

where $d=0.76$ and the values a , b , and c are the same as the values a , b , and c given in the statements and table for the brain. The facial skeleton is represented by a portion of the volume between two concentric elliptical cylinders. The portion of the volume that intersects the cranium and brain is excluded. The inequalities are:

$$\left(\frac{x}{a_1}\right)^2 + \left(\frac{y}{b_1}\right)^2 \leq 1, \left(\frac{x}{a_1-d}\right)^2 + \left(\frac{y}{b_1-d}\right)^2 \geq 1,$$

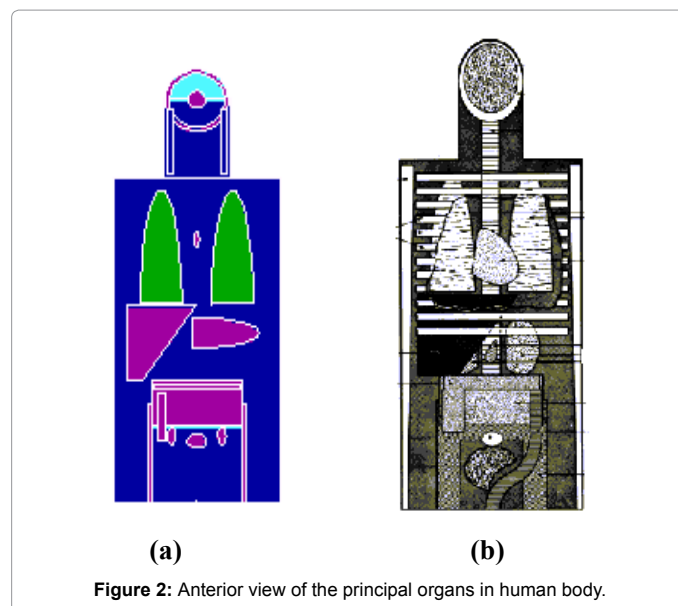


Figure 2: Anterior view of the principal organs in human body.

$$y \leq 0, C_T + z_1 \leq z \leq C_T + z_5,$$

$$\text{and } \left(\frac{x}{a_2}\right)^2 + \left(\frac{y}{b_2}\right)^2 + \left(\frac{z - [C_T + C_{H1}]}{c_2}\right)^2 > 1$$

The variables a_2 , b_2 , and c_2 correspond in numerical values with the variable expressions $(a+b)$, $(b+d)$, and $(c+d)$, respectively, in the statements defining the cranium and hence are not given below.

$$a_1=6.92, b_1=8.1, d=1.10, z_1=3.79, z_5=14.05$$

Pelvis: The pelvis is a portion of the volume between two nonconcentric elliptical cylinders. The inequalities defining the pelvis are

$$\left(\frac{x}{a_2}\right)^2 + \left(\frac{y - y_{02}}{b_2}\right)^2 \leq 1,$$

$$\left(\frac{x}{a_1}\right)^2 + \left(\frac{y - y_{01}}{b_1}\right)^2 \leq 1,$$

$y \geq y_{02}$, $0 \leq z \leq z_2$, and $y \leq y_1$ if $z \leq z_1$, where $a_1=9.75$, $b_1=11.07$, $a_2=10.35$, $b_2=11.76$, $Y_{01}=-3.72$, $y_{02}=-2.94$, $y_1=4.90$, $z_1=12.62$, $z_2=19.83$.

Spine: The spine is an elliptical cylinder given by

$$\left(\frac{x}{a}\right)^2 + \left(\frac{y - y_0}{b}\right)^2 \leq 1 \text{ and } z_1 \leq z \leq z_4$$

It is divided into 3 portions—an upper, middle, and lower—such that dose and absorbed fractions can be estimated separately for each portion. These divisions are formed by the planes $z=z_2$ and $z=z_3$.

$$A=1.73, b=2.45, y_0=5.39, Z_1=19.83, Z_2=31.64, Z_3=63.10, Z_4=72.91$$

Entrance surface dose

Two types of dosimeter are commonly used for estimating ESD to patients during X-ray examinations, namely Thermo-Luminescent Dosimeters (TLDs) and ionization chambers. TLDs have the advantage of being physically small, enabling them to be stuck directly and unobtrusively on the patient's skin with very little interference in patient mobility or comfort. They will fully measure the radiation backscattered from the patient, an essential component of the Entrance Surface Dose (ESD) and are unlikely to obscure useful diagnostic information. Ionization chambers, being more bulky and requiring connecting cables are usually difficult to attach in sufficiently close contact to the patient's skin to ensure complete measurement of the backscattered radiation, severely restrict patient mobility and cast interfering shadows on radiographs [12]. They are consequently not recommended for direct measurement of ESD. They can, however, be used to make measurements of the absorbed dose to air, in free air, on the axis of the X-ray beam without a patient or phantom present. Such measurements can be corrected using appropriate backscatter factors and the inverse square law to estimate the ESD. In previous study, Victoreen 4000M+ was used to evaluate the dose to patients during different diagnosis as part of implement QC program in diagnostic radiology [13]. TLDs are recommended for direct measurement of ESD and are available in a variety of physical forms and in different materials. The National Radiological Protection Board (NRPB) recommends individual chips or pellets of lithium fluoride or lithium borate [12]. TLDs dosimeters (Harshaw TLD100) is undertaken in this study for validation of ESD with the calculation using by MCNP4C. The TLDs were read using a

Harshaw 4500 TLD reader. The TLD energy response was 15% across the range 20–200 kVp, the uncertainty of measurement was estimated to be less than 10%. ESD is absorbed dose in soft tissue that would be measured at the point where the central axis of the x-ray beam enters the body. The five most frequently performed diagnostic radio-graphic examinations were included in the study; Skull, Chest, Abdomen, Pelvis and Lumper Spin. For each radiographic projection the mean patient weight was within the range of 70 kg. For each radiograph the tube potential, mAs, FSD, FFD, cassette size, patient weight and age were recorded. The image quality of all X-ray examinations included in the sample was satisfactory according to the radiologists of the department and fulfilled all image criteria set according to the European guidelines [14]. Radiographic condition used in definition of normalized organ dose is illustrated in Table 1 and Figure 3.

The contribution of backscattered radiation is to be included. ESD is related to the incident absorbed dose by the backscatter factor BSF thus,

$$ESD=(ID) (BSF)$$

BSF depends on the X-ray spectrum, the X-ray field size, the thickness of the patient and the distance between the center of the dosimeter and the surface [15]. The influence of this factor can be minimized by using a dosimeter of small volume directly attached to the patient's skin or by recessing the dosimeter in the surface of the phantom [16].

Organ	Exposure parameters		
	kVp	mA	Sec
Chest (PA)	50-60	100	0.7
Skull	50-60	40	1
Abdomen (AP)	60-70	40	2
Pelvis (AP)	70-80	40	2
Lumbar spine (AP)	60-80	60	2

Table 1: Radiographic condition used in definition of normalized organ dose.

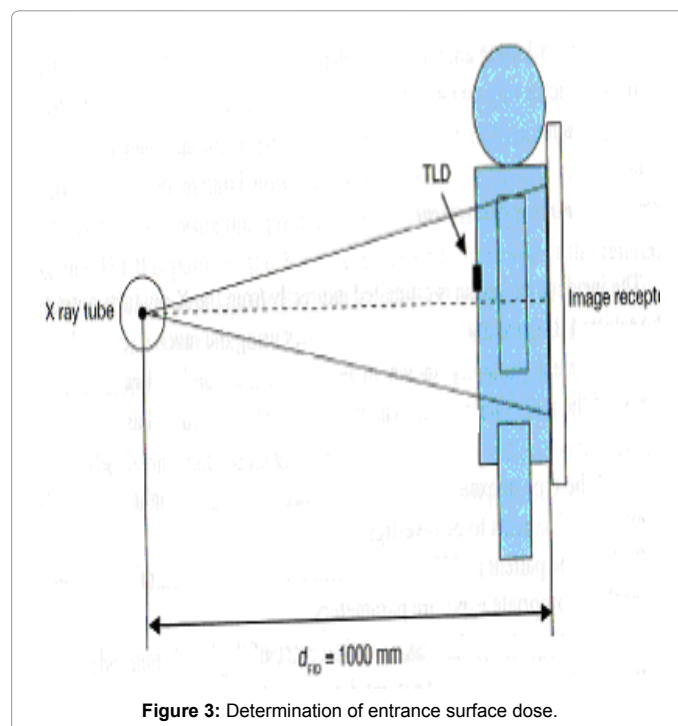


Figure 3: Determination of entrance surface dose.

Calculation of ESD from tube output

$$ESD = K_a (U, F) (100 \text{ cm}/FSD)^2 P_{it} \text{BSF}$$

Where

$K_a (U, F)$ is the tube output (mGy/mAs) at a distance of 100 cm from the focus with high voltage U and total filtration F.

FSD is the focus to skin distance cm.

P_{it} tube current-time product used mAs.

Results and Discussion

Table 2 presents the mean values and standard deviation of measured and, as well as the calculated ESD for Skull, Chest, Abdomen, Pelvis and Lumper Spin examinations. As shown in Table 2, the mean ESD ranged from approximately 0.23 to 0.57 mGy for chest, from 2.03 to 5.1 mGy for skull, from 2.58 to 3.54 mGy for abdomen, from 6.3 to 13.6 for pelvis and from 4.1 to 7.1 to lumbar spine. The ESD measured by TLD are slightly higher than ESD in all. The main source of the high values of the experimental results may come from many factors such as: the reproducibility of exposure (within 2% for one standard deviation), variations due to the experiment geometry, and variations of TLD sensitivities (within 10%, for one standard deviation) [16]. It

must be stressed that the TLD threshold dose not only depends on the annealing and measurement protocols used and the equipment available, but also on the particular batch of TLDs used for the ESD measurements. Therefore, more investigation should be done using other types of TLDs such as calcium Fluoride (CaF) dosimeters that are much more sensitive than LiF TLDs.

The correlation between ESD calculated and ESD measured by TLD in all radiographic procedures included in the study were: PA chest: 0.89%; AP abdomen: 0.96%; AP pelvis: 0.97%; AP lumbar spine: 1.03% and skull: 1.05%. Thus for all examinations studied, the correlation between calculated and measured doses was very high as shown in Table 2, Figures 4 and 5.

According to the European Commission (EC) and National Radiation Protection Board (NRPB), the mean ESD in all radiographic examinations being substantially lower than Guidelines dose reference levels (EC and NRPB Dose Reference Level). More attention should be taken for chest examinations, where, the mean ESD is two times higher than the DRL proposed by EC and DRLs recently proposed by NRPB [14,17] given in the Table 3 [17-20]. The practical and calculated data for each examination are compared with the data reported from different similar studies for each examination and presented in Figure 6.

Organ	kVp	Measured ESD	Error%	Calculated ESD	Error%
Chest (PA)	50-60	0.23-0.57	0.01-0.05	0.19-0.6	23-5.3
Skull	50-60	2.03-5.1	0.03-0.08	1.7-5.5	16.3-7.8
Abdomen (AP)	60-70	2.58-3.54	0.05-0.09	2.34-3.84	10.9-8.5
Pelvis (AP)	70-80	6.3-13.6	0.07-0.1	6.12-13.97	2.9-2.7
Lumbar spine (AP)	60-80	4.1-7.1	0.1-0.2	3.8-7.4	7.3-4.2

Table 2: ESD (mGy) measured and calculated for different examinations.

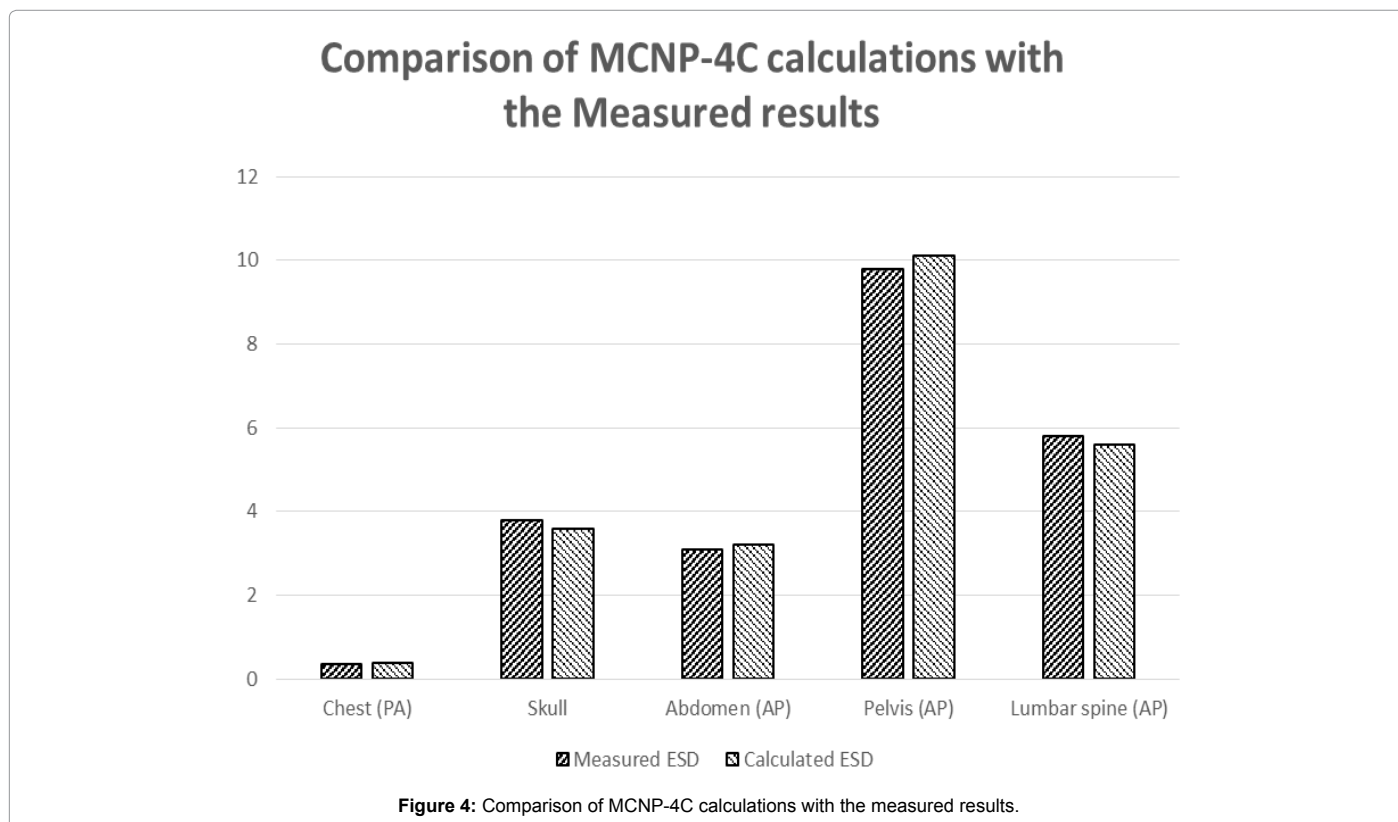


Figure 4: Comparison of MCNP-4C calculations with the measured results.

THE CORRELATION BETWEEN CALCULATED AND MEASURED DOSES

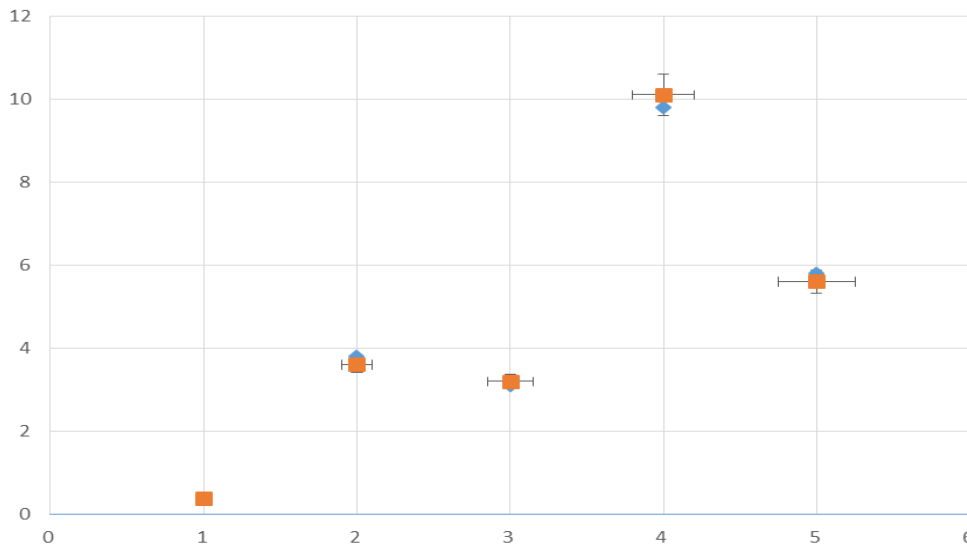


Figure 5: The correlation between calculated and measured ESD.

Organ	Egypt	UK [18]	DRL [17]	DRL _{EC} [14]	Gracee [1]	Romania [1]	Slovinia [1]	Italy [19]	Portogal [1]	Serbia [20]
Chest (PA)	0.35	0.16	0.2	0.3	0.69	1.7	0.23	0.57	0.31	0.4
Skull	3.8	3.9	--	--	3.5	11	--	7.38	7.27	1.15
Abdomen (AP)	3.1	6.0	6.0	--	----	---	---	---	----	----
Pelvis (AP)	9.8	4.4	-	10	12.5	13.2	3.8	7.77	----	2.0
Lumbar spine (AP)	5.8	6.1	-	10	18.9	17.6	6.9	8.9	5.95	4.4

Table 3: Comparison of mean values of ESD (mGy) in this study (Egypt) by several radiographic procedures surveyed in different countries.

Comparison of mean values of ESD (mGy) in this study (Egypt) by several radiographic procedures surveyed in different countries

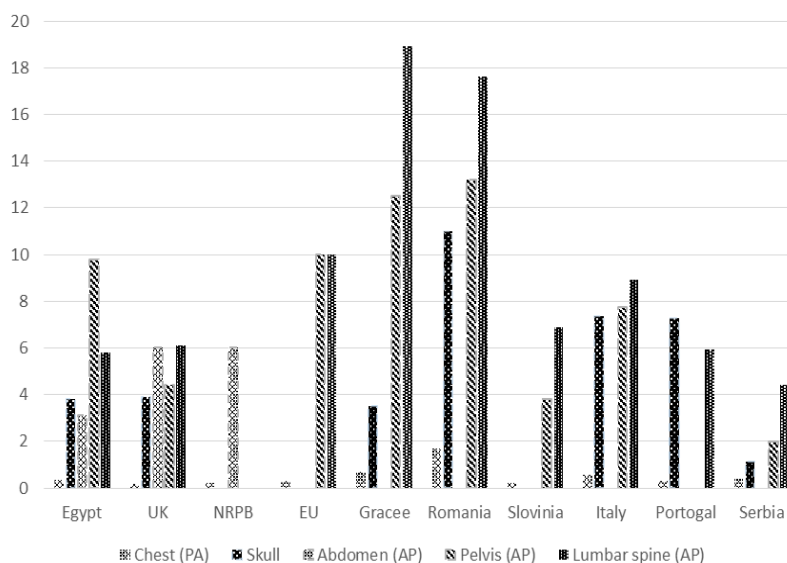


Figure 6: Comparison of mean values of ESD (mGy) in this study (Egypt) by several radiographic procedures surveyed in different countries.

From the data obtained in this study, radiodiagnostic facilities are required to implement a system for patient dose reviews based on comparisons with International, national and local Diagnostic Reference Levels (DRLs). This DRL can be verified through the Quality Assurance (QA) programme. The QA is important to assess the performance characteristics of X-ray, ensure optimal image quality and perform accurate diagnosis.

Conclusion

If a wide variety of clinical situations or exposure conditions need to be simulated, a mathematical representation of the patient and theoretical calculation of the mean organ doses may be more suitable. Theoretical calculations of organ doses passage of X-ray photons through the phantom. The parameter defining the X-ray beam can be easily modified so that the organ doses relative to exposure or surface absorbed dose can be calculated for any desired diagnostic X-ray field.

The present work aimed to present this simulation of human body depending on the description of the reference man given by ICRP 23 [3] with material composition taking from ICRP 89 [21] using Monte Carlo code MCNP4c. So the obtained results gave a useful tool for calculate ESD in diagnostic X-ray for different KVP and for any organ in the human body in few second which is an important way to estimate the dose received by the patient in every exposure.

Thus, Monte Carlo techniques dealt most of all the instrumental problems and provide reproducible results for any combination of the beam quality and the field size. Any range of Tissue-Air Ratios (TAR) values can be tabulated when the theoretical X-ray spectrum matches to the output spectrum of X-ray system used in practical studies.

References

- Ngachin M, Garavaglia M, Giovani C, Kwato Njock MG, Nourreddine A (2008) Radioactivity level and soil radon measurement of a volcanic area in Cameroon. *J Environ Radioact* 99: 1056-1060.
- Ron E (2003) Cancer risks from medical radiation. *Health Phys* 85: 47-59.
- Abbadly AG, Uosif MA, El-Taher A (2005) Natural radioactivity and dose assessment for phosphate rocks from Wadi El-Mashash and El-Mahamid Mines, Egypt. *J Environ Radioact* 84: 65-78.
- Alonso M, Barriuso T, Castañeda MJ, Díaz-Caneja N, Gutiérrez I, et al. (1999) Monte Carlo estimation of absorbed dose to organs in diagnostic radiology. *Health Phys* 76: 388-392.
- Briesmeister J (2000) MCNP - A General Monte Carlo N-Particle Transport Code Version4C Los Alamos National Laboratory LA1370914.
- FULEA D (2009) MONTE CARLO METHOD FOR RADIOLOGICAL X-RAY EXAMINATIONS. *Rom Journ Phys* 54: 629-639.
- http://www.ddmed.eu/_media/training_course:jarvinen_intro_to_patient_dose_quantities.pdf.
- Osei EK, Barnett R (2009) Software for the estimation of organ equivalent and effective doses from diagnostic radiology procedures. *J Radiol Prot* 29: 361-376.
- Massoud E (2005) MCNP Code in Assessment of the Variations of the Effective Dose with Torso Adipose Tissue Thickness. *Arab Journal of nuclear Sciences and Applications*.
- Shahbazi Gahrouei D (2006) Enternace Surface Dose Measurements for Routine X-Ray Examination in Chaharmahal and Bakhitiaria Hospital. *Iran J Radiation Res* 4: 29-34.
- Eckerman KF, Cristy M, Ryman JC (1996) The OR NL mathematical Phantom Series.
- http://www.hpa.org.uk/web/HPAweb&HPAwebStandard/HPAweb_C/1195733775699
- Diab HM (2004) Evaluation of Quality Control and Assurance Programme in Diagnostic Radiology. *International Eighth Conference of Nuclear Science and Applications* 2: 57-579.
- European Guidelines on quality criteria for diagnostic radiographic images. European Commission, EUR 16260 EN, 1996.
- Wall BF (1996) How to Assess the Dose to the Patient in Diagnostic radiology. 9th International Congress of the International Radiation Protection Association R-02.
- Meric N, Bor D, Buget N, Ozkirimli M (1998) The use of Monte Carlo Technique for the determination of Tissue-Air Ratios (TAR) in diagnostic energy range. *Physics Medica* 14.
- Hart D, Hillier MC, Wall BF (2002) Doses to patients from Medical X-ray examinations in the UK-2000 Review, National Radiation Protection Board (NRPB)-W14.
- Tsapaki V, Tsalafoutas IA, Chinofoti I, Karageorgi A, Carinou E, et al. (2007) Radiation Doses to patients undergoing standard radiographic examinations: a comparison between two methods. *The British Journal of Radiology* 80: 107-112.
- Padovani R, Contento G, Fabretto M, Malisan MR, Barbina V, et al. (1987) Patient doses and risks from diagnostic radiology in North-east Italy. *Br J Radiol* 60: 155-165.
- Olivera Ciraj, Srpko Markovic, Dusko Kosutic (2004) Patient Dose from Conventional Diagnostic Radiology Procedures in Serbia and Montenegro. *The Journal of Preventive Medicine* 12: 26-34.
- (2002) International Commission on Radiological Protection. *Ann ICRP*, Bergamon Press: ICRP Publication 89, Oxford, UK 32: 2002.